



FORESTRY SCIENCE

Assessing over decadal biomass burning influence on particulate matter composition in subequatorial Amazon: literature review, remote sensing, chemical speciation and machine learning application

ADRIANA GIODA, VINICIUS L. MATEUS, SANDRA S. HACON, ELIANE IGNOTTI, RUAN G.S. GOMES, MARCOS FELIPE S. PEDREIRA, JOSÉ MARCUS GODOY, RIVANILDO DALLACORT, ANA LÚCIA M. LOUREIRO, FERNANDO MORAIS & PAULO ARTAXO

Abstract: A study on aerosols in the Brazilian subequatorial Amazon region, Tangará da Serra (TS) and Alta Floresta (AF) was conducted and compared to findings in an additional site with background characteristics (Manaus, AM). TS and AF counties suffer from intense biomass burning periods in the dry season, and it accounts for high levels of particles in the atmosphere. Chemical characterization of fine and coarse particulate matter (PM) was performed to quantify water-soluble ions (WSI) and black carbon (BC). The importance of explanatory variables was assessed using three machine learning techniques. Average concentrations of PM in AF and TS were similar ($PM_{2.0}$, $17 \pm 10 \mu\text{g m}^{-3}$ (AF) and $16 \pm 11 \mu\text{g m}^{-3}$ (TS) and $PM_{10-2.0}$, $13 \pm 5 \mu\text{g m}^{-3}$ (AF) and $11 \pm 7 \mu\text{g m}^{-3}$ (TS)), but higher than the background site. BC and SO_4^{2-} were the prevalent components as they represented 27%–68% of particulates chemical composition. The combination of the machine learning techniques provided a further understanding of the pathways for PM concentration variability, and the results highlighted the influence of biomass burning for key sample groups and periods. $PM_{2.0}$, BC, and most WSI presented higher concentrations in the dry season, providing further support for the influence of biomass burning.

Key words: biomass burning, CIT, particulate matter, random forests, secondary inorganic aerosol.

INTRODUCTION

The Brazilian Amazon is the world's largest tropical-forest reserve representing approximately one-third of forests on the globe. Forest exploitation in the Amazon, has significantly increased in the last few decades since the timber supply in Southern Brazil has come to exhaustion. Moreover, infrastructure developments, such as the construction of roads, hydroelectric power plants, and large settlements, have also become increasingly

common in the Amazon. Additionally, current deforestation practices, often linked to wildfire, degradation caused by natural resources extraction, and also by new settlements disorderly implemented, are among the main causes of anthropic disturbance in forest sites. These practices, along with natural forest events, have a profound impact on ecological damage and carbon emissions (Bullock et al. 2020).

The Amazon region has a wet tropical climate, with two well-defined seasons: the

rainy summer season and the dry winter season. Biomass burning is often observed over the Amazon in the dry season, and this is the main anthropogenic source of particle and gas emissions. Huge amounts of greenhouse gases and aerosol particles are released during wildfire events, and they threaten biodiversity and local population. In addition, intense carbon emissions have a negative impact on the Amazon climate by altering biogeochemical processes (Cammelli et al. 2020, Covey et al. 2021, Silva et al. 2021). Cloud droplets are formed by water vapor condensation in aerosol particles emitted from fire events. These particles can affect cloud properties and, consequently, atmospheric dynamics and radiative balance (Takeishi et al. 2020). Therefore, large amounts of aerosol particles from forest fire events contribute to cloud condensation nuclei (CCN) formation in small water-vapor volumes. This process decreases the possibility of large droplets' formation and, consequently, contributes to cloud longevity (Twomey 1959, Albrecht 1989, Liu & Daum 2002, Takeishi et al. 2020). Aerosol particles have a major influence on health due to their size range and chemical composition variability. Forest wildfire in the dry season has an adverse effect on human health in the Amazon region since it increases the emission of PM. This air quality degradation spreads to other regions due to wind action raising the number of hospitalizations and death (especially children and elderly), associated with breathing and cardiovascular diseases (Butt et al. 2020, Rocha & Sant'Anna 2022, Urrutia-Pereira et al. 2021). Fire events influence the biogeochemical cycles of trace elements, affecting essential nutrients, such as P, N, K, C and S, causing environmental imbalance. Acid deposition in ecosystems is a result of biomass burning, influenced by acetic and formic acid emissions, and associated to photochemical formation of NO_3^- and SO_4^{2-} (Costa

et al. 2022). Furthermore, aerosol particles emission from biomass burning is not only a regional but also a global concern as biomass burning plumes are capable of traveling long distances affecting climate and health at the global scale.

Mato Grosso is among the states that are most affected by wildfire events in the Brazilian Amazon region. Since the 1970s, this state has been undergoing a sharp transformation in its territory influenced by the opening of large agricultural areas, which is detrimental to the Amazon and *Cerrado* biomes. This deforestation process drives the expansion of frontiers for agricultural and grazing activities, as well as boosts urbanization processes. However, deforestation and wildfire rates have not changed in this same proportion over the years, mainly the ones observed in the dry season, especially between July and November (De Oliveira et al. 2022).

The aim of the present study was to determine the chemical composition of aerosols collected in two regions in Mato Grosso State: Alta Floresta (AF) and Tangará da Serra (TS) affected by the burning of different biomass types: pasture and forest, respectively. To ensure the objectives our methodology is based on aerosol chemistry and use of machine learning algorithms (Conditional Inference Trees – CIT, Random Forests, and Hierarchical Clustering Analysis – HCA). The current study also contributes about the collected data of these regions. Additionally, we have included information on a third Amazonian site (Manaus), which serves as a background site, to enrich the discussion and long-term comparison of AF and TS.

MATERIALS AND METHODS

Sampling sites

Sampling was carried out in Tangará da Serra (TS, 14 ° 37' 10" S, 57 ° 29' 09" W, 427 m asl) and Alta

Floresta (AF, 9 ° 52 '32" S, 56 ° 5' 10" W, 283 m asl) counties, Mato Grosso (MT) State, subequatorial Amazon region (Figure 1). These two sites belong to a region susceptible to drought and rain cycles that alter the local air pollution levels affecting the quality of life. These sites are located in the pollution dispersion path that originates from both the Brazilian Amazon and neighboring countries (Freitas et al. 2005, Martin et al. 2010).

Tangará da Serra is located in Southwestern Mato Grosso State. Wildfire events influences the community air quality and it is partially attributed to sugarcane leaves burning by the surrounding neighborhood, typically after the harvest season. Tangará da Serra community developed from "poaia" (*Cephaelis ipecacuanha*) forest exploitation because of its medicinal properties. Later on, loggers were attracted to

this region initiating the forest devastation. At that time, agriculture was the main activity and practiced on open land. Currently it remains as the main activity in the area with soybean and sugarcane being the prevailing cultures. Additionally, livestock is currently in expansion in the region.

Alta Floresta is located in Northern Mato Grosso State, 800 km far from TS and its terrain has typical characteristics of the Amazon rainforest. Wildfire events in this region originates from pasture and forest burning. The local community was settled during the Amazon Rubber Boom in the 1970s and the region underwent further development during the gold rush in the 1980s (Hacon et al. 2000, Lacerda et al. 2004). Nowadays, the local economy is driven by cattle breeding, timber industry, and

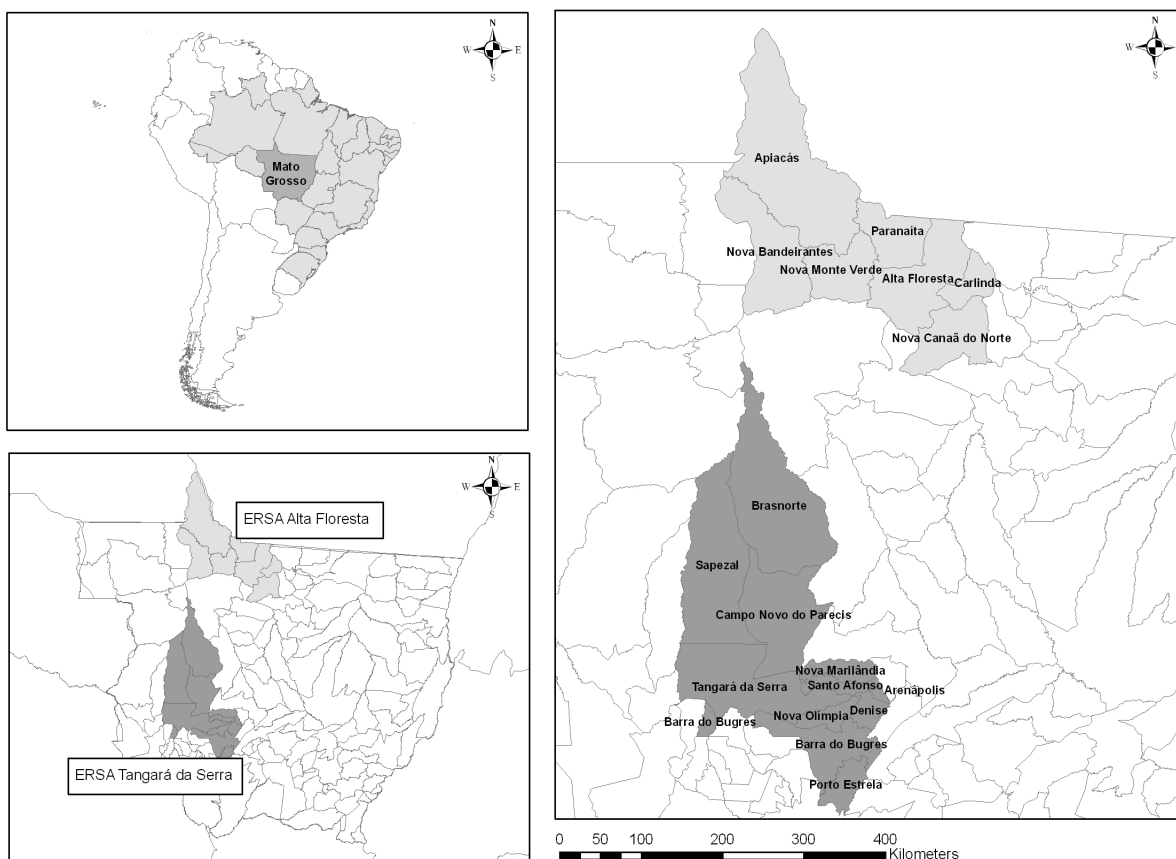


Figure 1. Communities of Alta Floresta and Tangará da Serra, state of Mato Grosso, subequatorial Amazon.

dairy production. Adding to these two regions (AF and TS), air pollution concentrations were compared to samples collected in a remote area (Rebio Cuieiras, ZF2 - 2°35'22 "S, 60°06'55" W), approximately 80 km from Manaus, AM, to assess air pollution magnitude in AF and TS. This region is covered by dense rainforest, and accounts for low anthropogenic impact.

Particles sampling

Particulate matter (PM) samples were continuously collected for 24 h or 48 h, using stacked filter units (SFUs) fitted to PM₁₀ inlet, which separates particles into coarse (2.0–10 µm in aerodynamic diameter, PM_{10-2.0}) and fine (diameter smaller than 2.0 µm, PM_{2.0}) fractions. Polycarbonate filters, 47 mm in diameter (Millipore Corporation, Billerica, MA, USA): coarse, 8-µm in diameter, and fine pore size, 0.4-µm in diameter, were used in the aforementioned system. The flow rate was approximately 16 L min⁻¹. In total, 99 fine and coarse samples were collected in Alta Floresta, 96 fine and coarse samples were collected in Tangará da Serra, and 50 fine and coarse samples were collected in Manaus and used in the current study (Table I).

Analyses

Particle mass was determined through gravimetric analysis. Filters were weighed and conditioned at 21.5 °C ± 2 °C, at 42.5% ± 5% humidity, before and after sampling. The filters were weighed on an analytic scale (Mettler scale) every day until no more variations were found in the readings. The criteria was based on three consecutive measurements whose standard deviation did not vary larger than 0.00002 g.

Black carbon (BC) concentration was determined through the light reflectance technique (Andreae et al. 1984). The BC concentration is proportional to the reflection

absorbance of the light source illuminating the sample. Filters loaded with known amounts of BC resulting from acetylene combustion were the reference samples.

Polycarbonate filters were extracted with 10.0 mL ultrapure water and stirred for 10 minutes. Subsequently, samples were filtered in 0.45 µm membranes and analyzed. Samples ionic concentrations were determined using the Dionex ion chromatography system (model DX-120, for cations; and model ICS-2000, for anions). Six anions: CH₃COO⁻ (acetate), HCOO⁻ (formate), Cl⁻, SO₄²⁻, NO₃⁻ and PO₄³⁻; and five cations: NH₄⁺, Ca²⁺, Mg²⁺, K⁺ and Na⁺ were measured. Eluent KOH concentration ranging from 10 to 52 mmol L⁻¹ was used for anions analysis by using IonPac AS-19 (4 mm) column. IonPac CS-12A (4 mm) column, and H₂SO₄ at 10 mmol L⁻¹ were used as eluent for cations. Samples were analyzed in triplicate and the detection limit of each ion was computed as the blank average, plus two times the blank standard deviation. A calibration check with external standards was performed to ensure ± 5% accuracy for cations and anions.

Ultrapure filtered and unfiltered water was analyzed before extraction to assess and ensure the quality control. Blank filters were simultaneously processed with sample filters. Mean values recorded for species in the blanks were subtracted from each sample filter. A calibration check was performed in intervals of 10 samples to ensure a relative standard deviation not higher than 10%. Recovery efficiency rates were higher than 90%.

Source apportionment

Hypothesis testing

Mann–Whitney ($p < 0.05$) and Pearson's tests were used to determine similarities and correlations among samples and sites, respectively. These statistical analysis methods were conducted in

GraphPad Prims 6.0 (GraphPad Software, Inc., San Diego, CA).

Left-censored data

Dealing with left-censored data is a frequent challenge in environmental research. It is well known that simple number imputation or variable removing approaches lead to biased conclusions (Palarea-Albaladejo & Martín-Fernández 2015). Information provided by left-censored data was processed in R package *zComposition*, based on the compositional approach (Palarea-Albaladejo & Martín-Fernández 2015).

Conditional Inference Trees (CIT)

PM mass concentration may be expressed based on its chemical components. Undoubtedly, there are other factors, such as meteorology, that interact with chemical components (e.g., the effect of seasonality) and play an important role in PM concentration. Therefore, CIT analysis was carried out by considering chemical speciated PM components and a dichotomous variable called "Season" which assumes binary value (0 = Wet and 1 = Dry). A conditional distribution can be written by m -dimensional covariate $X = (X_1, X_2, \dots, X_m)$ if PM mass concentration is taken as variable Y response:

$$D(Y|X) = D(Y|X_1, X_2, \dots, X_m) = (Y|f(X_1, X_2, \dots, X_m))$$

Wherein, f is a function of the covariate. The binary partitioning algorithm is based on the non-negative integer valued case weight vector, given a population ϕ_n with n cases. The case weight vector w assumes zero value for observations for each node of the tree; otherwise, they are not elements of the hole node and nonzero integer. The analysis was carried out by using function *ctree* in the R package *party* (Hothorn et al. 2006).

Random forests

Random forests are a nonlinear and nonparametric statistical method that is the further development of the so-called bagging or bootstrap aggregation (Breiman 2001). Random forests are an ensemble learning method that operates from a decision tree architecture. This technique is a major data analysis tool used in many scientific fields, and it can be particularly useful when it comes to small datasets that carry a large amount of information, the so-called "small n large p " problems. However, the method is not reliable when predictors varies by different orders of magnitude or in number of categories (Strobl et al. 2007). In this study, the selection of variables was based on a CIT logic origin framework rather than in traditional classification analysis and regression trees (CART) (Strobl et al. 2007). The analysis was performed using the *cforest* function in the R package *party* (Hothorn et al. 2005, Strobl et al. 2007, 2008).

Hierarchical clustering analysis (HCA)

Hierarchical clustering analysis (HCA) aims at finding the distance between samples that is represented in a two-dimensional space (i.e., dendrogram) and based on a specified metric. It is of widespread use in data analysis and it provides a simple and intuitive graphical output. Although HCA have these appealing characteristics, the clusters accuracy and reproducibility can be questionable. To mitigate this drawback the multistep-multiscale bootstrap resampling was used and implemented using the *pvclust* package available in R language (Suzuki & Shimodaira 2006). The aim of the multistep-multiscale bootstrap resampling is to ensure data structure reliability based on approximately unbiased (AU) p-value estimates, rather than on regular bootstrap probability (BP) estimates.

RESULTS

Particulate matter concentrations

Supplementary Material - Figure S1 displays time series of the particulate matter. The figure includes two sampling sites (TS and AF) and both seasonal campaigns. A closer inspection of the aerosol frequency distributions, indicates that concentrations ranged between 6 and 15 $\mu\text{g m}^{-3}$ in both particle sizes. The mean fine particle concentrations at TS and AF sites were similar (17 ± 10 in TS and $16 \pm 11 \mu\text{g m}^{-3}$ in AF), and significantly differs from the background site (i.e., 1.35 ± 0.93 in Manaus). However, $\text{PM}_{10-2.0}$ was slightly lower in TS ($11 \pm 7 \mu\text{g m}^{-3}$) than in AF ($13 \pm 5 \mu\text{g m}^{-3}$) and, again, it was higher than in Manaus (4 ± 2) (Table I).

Chemical composition of particulate matter

Mean ionic compositions (the sum of cation and anion concentrations) in $\text{PM}_{2.0}$ were 1.7 $\mu\text{g m}^{-3}$ (TS), 2.0 $\mu\text{g m}^{-3}$ (AF), and 0.4 $\mu\text{g m}^{-3}$ (Manaus). These values represent approximately 10%–13% of total particle mass for TS and AF, and approximately 29% for Manaus. Mean concentrations in $\text{PM}_{10-2.0}$ were 0.84 $\mu\text{g m}^{-3}$ (TS), 0.79 $\mu\text{g m}^{-3}$ (AF), and 0.37 $\mu\text{g m}^{-3}$ (Manaus). These values accounts for 6%–10% of total particle mass. BC represented approximately 8%–9% of the total fine concentrations and 1%–2% of the total $\text{PM}_{10-2.0}$ concentrations. The black carbon and SO_4^{2-} represented 30%–68% of the total PM concentrations at both TS and AF sampling sites. Such behavior is similar to that observed in Manaus (27%–63%) (Figure S2).

Influence of biomass burning

PM concentrations have indicated interesting differences. The highest PM concentrations were observed in the dry season (Table I), from June 1 to October 31 (Echalar et al. 1998). The mean $\text{PM}_{2.0}$ concentrations, at both sampling sites,

were approximately two times higher in the dry (18–20 $\mu\text{g m}^{-3}$) compared to the wet season (7 $\mu\text{g m}^{-3}$). Similarly, concentrations in Manaus were higher in the dry season (Table I). Despite these similar characteristics, the concentration levels at Manaus were much lower than at TS and AF.

PM level measured in the present study were considerably lower than those reported by previous studies. The first study performed in AF (Aug/Set 1992–1993) recorded mean concentrations of 84 (± 54) $\mu\text{g m}^{-3}$ for fine particles (Hacon et al. 1995). This value is four times higher than reported in our study. A second investigation (1992–1995) showed that fine particle concentration had decreased, compared to the first study, to 47 (± 41) $\mu\text{g m}^{-3}$ in the dry season and to 5.5 (± 3.5) $\mu\text{g m}^{-3}$ in the wet season (Echalar et al. 1998). The next study (1996 and 1998) showed slightly higher fine particle concentrations compared to Echalar work (et al. 1998). The values were 63 (± 55) $\mu\text{g m}^{-3}$ in the dry season and 9.9 (± 9.9) $\mu\text{g m}^{-3}$ in the rainy season, on average (Maenhaut et al. 2002). Measurement performed between 2004–2005, showed a subsequent decrease in the average fine particle levels, corresponding to 33–44 $\mu\text{g m}^{-3}$ during the biomass burning period, and 2.5 $\mu\text{g m}^{-3}$ when there were no fire events (Carmo et al. 2010, Ignotti et al. 2010). While these available studies significantly enhance our knowledge of the PM behavior at AF, the same does not stand in the same proportion at TS. The measured mean fine particle concentration, in the dry season, during the 1990s, was as high as 400 $\mu\text{g m}^{-3}$ (Artaxo et al. 1988, Maenhaut et al. 1998) and dropped between 210–258 $\mu\text{g m}^{-3}$ in the early 2000s (Carmo et al. 2010, Ignotti et al. 2010). In 2004–2005, the estimated mean fine particle concentration in the dry season was 31 (± 29) $\mu\text{g m}^{-3}$ (Carmo et al. 2010, Ignotti et al. 2010). Maximum concentrations recorded in this study ranged from 41 to 56 $\mu\text{g m}^{-3}$. Overall, the average

Table I. Average, standard deviation, and range concentrations of the aerosol samples collected in Alta Floresta, Tangará da Serra, and Manaus. Dry season refers to biomass burning period (June 1 to October 31) and wet season for the other months.

		Alta Floresta		Tangará da Serra		Manaus	
		Coarse	Fine	Coarse	Fine	Coarse	Fine
N	Whole	99	99	96	96	50	50
	Wet	30	30	21	21	31	31
	Dry	69	69	75	75	19	19
PM ($\mu\text{g m}^{-3}$)	Whole period Range	13.3 \pm 5.5 (3.5-36.0)	16.8 \pm 9.9 (0.8-40.9)	11.2 \pm 7.4 (2.4-40.5)	15.9 \pm 11.3 (2.7-55.9)	3.7 \pm 2.0 (0.6-9.0)	1.5 \pm 0.9 (0.38-4.2)
	Wet season	13.2 \pm 3.5	7.4 \pm 2.6	6.0 \pm 5.7	7.2 \pm 3.9	4.5 \pm 1.8	1.1 \pm 0.6
	Dry season	13.4 \pm 6.3	19.7 \pm 9.2	12.7 \pm 11.4	18.3 \pm 11.5	2.3 \pm 1.5	2.0 \pm 1.1
BC* ($\mu\text{g m}^{-3}$)	Whole period Range	0.17 \pm 0.09 (0.05-0.55)	1.39 \pm 0.78 (0.30-2.90)	0.21 \pm 0.16 (0.04-0.62)	1.36 \pm 0.90 (0.26-3.73)	0.07 \pm 0.06	0.20 \pm 0.13
	Wet season	0.14 \pm 0.03	0.68 \pm 0.22	0.09 \pm 0.08	0.61 \pm 0.29	0.06 \pm 0.017	0.09 \pm 0.06
	Dry season	0.19 \pm 0.11	1.69 \pm 0.72	0.24 \pm 0.19	1.56 \pm 0.89	0.07 \pm 0.02	0.32 \pm 0.20
Acetate (ng m^{-3})	Whole period Range	49.1 \pm 45.2 (nd-380.0)	34.0 \pm 29.5 (nd-300.0)	56.5 \pm 29.5 (nd-90.1)	55.4 \pm 50.5 (nd-140.2)	21.9 \pm 19.5 (nd-86.7)	52.9 \pm 67.2 (nd - 281.1)
	Wet season	77.9 \pm 76.5	50.8 \pm 43.8	56.5 \pm 29.5	76.1 \pm 44.1	19.5 \pm 16.4	60.0 \pm 79.1
	Dry season	36.0 \pm 34.0	27.3 \pm 13.4	nd	3.6 \pm 0.5	26.9 \pm 24.8	44.5 \pm 43.6
Formate (ng m^{-3})	Whole period Range	30.1 \pm 29.5 (nd-360.0)	43.9 \pm 42.9 (nd-320.1)	12.1 \pm 8.6 (nd-41.1)	30.3 \pm 20.8 (nd-80.1)	34.8 \pm 47.6 (nd-204.4)	67.0 \pm 82.1 (nd - 406.1)
	Wet season	37.3 \pm 32.3	36.3 \pm 0.23.9	9.4 \pm 6.7	13.3 \pm 12.2	31.9 \pm 51.3	56.0 \pm 61.0
	Dry season	28.4 \pm 25.4	47.0 \pm 41.6	13.0 \pm 9.0	32.5 \pm 20.3	38.9 \pm 33.7	93.0 \pm 113
Cl⁻ (ng m^{-3})	Whole period Range	62.1 \pm 61.4 (nd-520.9)	59.4 \pm 49.5 (nd-557.0)	7.8 \pm 7.5 (nd-42.3)	8.6 \pm 7.8 (nd-60.1)	30.9 \pm 47.6 (nd-291.4)	4.6 \pm 5.8 (nd-34.3)
	Wet season	107.0 \pm 99.0	126.8 \pm 118.5	5.2 \pm 4.5	5.4 \pm 4.0	41.8 \pm 56.8	3.3 \pm 3.1
	Dry season	42.3 \pm 42.0	35.3 \pm 27.1	8.5 \pm 7.9	9.4 \pm 6.3	11.4 \pm 4.8	7.2 \pm 8.5
NO₃⁻ (ng m^{-3})	Whole period Range	127.1 \pm 127.7 (nd-940.0)	59.7 \pm 58.5 (nd-640.0)	75.5 \pm 70.2 (nd-352.0)	59.4 \pm 50.8 (nd-530.5)	104.0 \pm 300.7 (nd-1958)	4.7 \pm 4.3 (nd-20.6)
	Wet season	134.6 \pm 81.3	90.8 \pm 89.5	17.3 \pm 14.9	40.1 \pm 38.1	121.5 \pm 358.3	4.0 \pm 3.3
	Dry season	124.2 \pm 120.5	54.1 \pm 46.3	91.7 \pm 89.5	64.6 \pm 48.7	6.5 \pm 8.4	6.4 \pm 6.4

Table I. Continuation.

PO_4^{3-} (ng m^{-3})	Whole period Range	53.1 \pm 40.6 (nd-190.1)	60.3 \pm 23.7 (nd-235.6)	16.2 \pm 9.9 (nd-480.2)	12.2 \pm 7.6 (nd-41.0)	29.7 \pm 16.9 (nd-84.2)	1.3 \pm 1.4 (nd-4.8)
	Wet season	55.0 \pm 44.2	87.7 \pm 72.2	8.2 \pm 4.5	14.9 \pm 8.4	36.5 \pm 15.1	1.6 \pm 1.3
	Dry season	52.1 \pm 32.6	48.4 \pm 46.3	18.5 \pm 9.9	11.2 \pm 7.2	17.6 \pm 12.7	0.81 \pm 1.43
SO_4^{2-} (ng m^{-3})	Whole period Range	102.7 \pm 85.9 (10.0-550.2)	895.1 \pm 646.8 (10.2-2930)	235.2 \pm 225.7 (10.1-1660)	684.0 \pm 523.7 (10.0-1920.1)	42.3 \pm 41.9 (1.3-209.9)	173.8 \pm 97.6 (32.3-507.8)
	Wet season	104.0 \pm 94.0	387.0 \pm 359.0	185.8 \pm 158.0	141.7 \pm 120.7	51.4 \pm 49.0	152.2 \pm 82.4
	Dry season	102.2 \pm 55.4	1105.6 \pm 566.0	409.3 \pm 352.0	833.9 \pm 482.3	26.2 \pm 16.1	213.4 \pm 115.6
Na^+ (ng m^{-3})	Whole period Range	93.2 \pm 91.5 (nd-710.3)	62.0 \pm 61.5 (nd-351.0)	53.6 \pm 50.5 (nd-210.6)	72.1 \pm 62.5 (nd-350.7)	35.5 \pm 36.2 (nd-117.3)	16.3 \pm 10.6 (nd-49.8)
	Wet season	75.1 \pm 65.7	39.2 \pm 36.6	36.6 \pm 34.6	44.8 \pm 21.2	37.5 \pm 38.3	11.9 \pm 5.9
	Dry season	101.7 \pm 101.2	71.8 \pm 69.5	58.7 \pm 58.0	79.1 \pm 45.1	31.9 \pm 32.7	25.9 \pm 12.9
K^+ (ng m^{-3})	Whole period Range	86.1 \pm 55.5 (nd-240.4)	288.4 \pm 209.6 (nd-910.0)	85.1 \pm 70.9 (nd-420.7)	257.0 \pm 249.3 (10.0-600.0)	42.6 \pm 27.2 (1.1-95.0)	25.9 \pm 22.0 (3.8-86.2)
	Wet season	110.9 \pm 68.0	80.0 \pm 69.2	108.7 \pm 83.0	57.0 \pm 41.4	54.3 \pm 23.0	18.0 \pm 16.2
	Dry season	73.2 \pm 43.2	351.8 \pm 196.5	78.3 \pm 71.3	312.3 \pm 108.9	21.9 \pm 21.4	41.4 \pm 23.4
Mg^{2+} (ng m^{-3})	Whole period Range	28.8 \pm 13.9 (nd-71.0)	15.7 \pm 12.5 (nd-70.1)	36.0 \pm 28.9 (nd-160.2)	21.8 \pm 15.8 (nd-80.7)	5.5 \pm 4.8 (nd-25.8)	1.5 \pm 1.5 (nd-6.1)
	Wet season	20.0 \pm 9.0	4.8 \pm 1.3	11.1 \pm 8.9	18.6 \pm 11.5	6.6 \pm 5.3	1.3 \pm 1.4
	Dry season	32.2 \pm 14.1	17.1 \pm 12.6	43.2 \pm 23.8	22.8 \pm 16.8	3.7 \pm 3.1	1.75 \pm 1.65
Ca^{2+} (ng m^{-3})	Whole period Range	83.7 \pm 60.0 (nd-281.0)	62.0 \pm 43.1 (nd-290.1)	119.0 \pm 80.6 (nd-440.4)	49.4 \pm 39.5 (nd-84.5)	8.1 \pm 8.0 (nd-42.2)	3.7 \pm 4.0 (nd-21.3)
	Wet season	33.6 \pm 28.6	21.2 \pm 18.2	53.9 \pm 24.6	43.6 \pm 22.0	9.0 \pm 8.7	4.0 \pm 4.4
	Dry season	90.2 \pm 58.2	74.6 \pm 40.7	124.6 \pm 81.4	51.4 \pm 41.5	5.8 \pm 5.6	3.12 \pm 3.24
NH_4^+ (ng m^{-3})	Whole period Range	73.2 \pm 60.5 (nd-423.2)	464.3 \pm 321.1 (nd-1200)	146.1 \pm 137.8 (nd-701.5)	414.1 \pm 288.2 (nd-1320)	1.2 \pm 1.0 (nd-4.8)	43.4 \pm 25.8 (nd-96.6)
	Wet season	130.6 \pm 102.4	121.2 \pm 116.5	254.2 \pm 152.2	176.6 \pm 121.6	1.4 \pm 1.0	37.7 \pm 24.6
	Dry season	40.1 \pm 33.4	599.4 \pm 267.5	100.5 \pm 92.2	434.2 \pm 189.7	0.9 \pm 0.8	61.7 \pm 21.8

nd: below of detection limits; *from Arana & Artaxo 2014.

fine particle concentrations indicate a decrease in the last few decades, in both AF and TS sites.

A significant difference ($p < 0.05$) in $PM_{10-2.0}$ concentrations between the dry ($13 \pm 11 \mu\text{g m}^{-3}$) and the wet ($6 \pm 6 \mu\text{g m}^{-3}$) seasons was observed in TS, however, the same did not stand for AF (13.4 and $13.2 \mu\text{g m}^{-3}$) (Table I). Differences between the dry and the wet seasons resulted from the fact that the dry period at 2008 in AF extended for longer than in TS, thus resulting in greater soil-particle resuspension. In 1992–1993, high coarse particle ($260 \pm 180 \mu\text{g m}^{-3}$) concentrations were measured in AF in the dry season, with extreme values as high as $600 \mu\text{g m}^{-3}$ (Hacon et al. 1995, Artaxo et al. 1994). Between 1992 and 1998, mean coarse particle concentrations in AF ranged between 34 to $37 \mu\text{g m}^{-3}$ in the dry season and 15 to $16 \mu\text{g m}^{-3}$ in the wet season (Echalar et al. 1998, Maenhaut et al. 2002). Similar to what was observed for the fine fraction, there has been a decrease in coarse particulate matter concentrations in recent decades. A different scenario was identified in Manaus since coarse particle concentrations were higher in the wet season ($4.5 \mu\text{g m}^{-3}$) than in the dry season ($2.4 \mu\text{g m}^{-3}$).

Biomass burning in Brazil is continuously monitored by satellites from the National Institute for Space Research (INPE) network. According to data provided by INPE, one of the lowest numbers of fire events in Mato Grosso State was registered in 2008. A biomass burning reduction trend has been observed in AF since 2004, but the same trend has not been observed in TS (Figure S3). An increase in the number of fire events is also associated with longer drought periods, as observed in 2010.

The mean BC concentration in $PM_{2.0}$ during the dry season (1.6 – $1.7 \mu\text{g m}^{-3}$) was approximately three times higher compared to the wet season (0.6 – $0.7 \mu\text{g m}^{-3}$) (Table I). The mean BC concentration in $PM_{10-2.0}$ was $0.2 \mu\text{g m}^{-3}$, with half

this value accounting for the wet season and half for the dry season ($0.1 \mu\text{g m}^{-3}$, each). Black carbon accounted for more than 40% of $PM_{2.0}$ and 20% of $PM_{10-2.0}$. Furthermore, this finding showed a close correlation ($r = 0.95$) between BC and $PM_{2.0}$. The BC: $PM_{2.0}$ ratio, in average, was within similar range (5 to 14%): $9\% \pm 2\%$ for both AF and TS. The BC: $PM_{2.0}$ pattern in AF was different from that observed in previous studies that recorded higher variability and means (Echalar et al. 1998).

K^+ in the current study ranged from 1.6% to 1.7%, which are similar to that found in plants (1.8%) (Bowen 1979). The mean recorded ratios ranged from 7 to 8 in the dry season and from 0.9 to 1.1 in the wet season and there were close correlations between BC and K^+ ($r = 0.75$ – 0.85).

Secondary inorganic aerosol and neutralization effects

The secondary inorganic aerosol fraction (SIA) is an important PM component, and it is calculated by the sum of SO_4^{2-} , NO_3^- and NH_4^+ . SIA represented approximately 7.1% of $PM_{2.0}$ at TS ($1.1 \mu\text{g m}^{-3}$) and 9.2% of $PM_{2.0}$ at AF ($1.4 \mu\text{g m}^{-3}$). On the other hand, the mean rate for $PM_{10-2.0}$ was 4.9% at TS ($0.39 \mu\text{g m}^{-3}$) and 1.9% at AF ($0.25 \mu\text{g m}^{-3}$). SIA was more representative for $PM_{2.0}$ (15%) in Manaus and it presented similar values to the ones at TS (4%), recorded for $PM_{10-2.0}$. Taking into account the seasonal basis, SIA concentrations in $PM_{2.0}$ were four to six times higher in the dry than in the wet season. No significant differences were observed for $PM_{10-2.0}$. Manaus showed no seasonal variations in the two assessed particle sizes. SIA showed a close correlation to $PM_{2.0}$ ($r = 0.75$). Ammonium sulfate $(\text{NH}_4)_2\text{SO}_4$ presented higher concentrations (0.9 – $1.2 \mu\text{g m}^{-3}$) in $PM_{2.0}$ than ammonium nitrate, NH_4NO_3 ($0.08 \mu\text{g m}^{-3}$). Although $(\text{NH}_4)_2\text{SO}_4$ concentrations were much higher in the dry season than in the wet season, there were no significant changes in NH_4NO_3 levels. SIA plays a key role in quality of the

air, climate change and, more specifically, in ecosystems' acidification. Mean BC:SIA ratio was higher than 1 for $PM_{2.0}$, but it was lower than 1 for $PM_{10-2.0}$ in the current research.

The neutralization ratio (NR) was calculated as $[NH_4^+]/[SO_4^{2-}] + [NO_3^-]$ to assess PM acidity. Annual and seasonal NRs, at both AF and TS sites, ranged from 0.2 to 0.5 and such finding indicates no neutral particles. $NO_3^-:SO_4^{2-}$ ratios showed inorganic ion prevalence in acidity outcomes. This ratio also pointed out nitrogen and sulfur mobile versus stationary sources in the atmosphere, respectively (Arimoto et al. 1996). We herein observed sulfate sources prevalence, since mean $NO_3^-:SO_4^{2-}$ ratios were lower than 1. Seasonal variation in $NO_3^-:SO_4^{2-}$ ratios recorded for $PM_{2.0}$ were observed, with the lowest ratios recorded in the dry season (0.08-0.20) and the highest ratios in the wet season (0.9). The $NO_3^-:SO_4^{2-}$ ratios for $PM_{10-2.0}$ were close to, or higher than, 1, and seasonality was not observed. A similar $NO_3^-:SO_4^{2-}$ ratios dynamics observed in AF and TS was also observed in Manaus.

Stochastic models

Coarse Mode: Alta Floresta

CIT consisted of 7 nodes, including 4 terminal nodes (Figure 2). BC concentration was the most important splitting variable for the root node. However, other water-soluble ions, such as Mg^{2+} , Ca^{2+} and K^+ , were also highly important, due to the emission of vegetation in the region. Release of various ions to the atmosphere in particulate matter occurs during transpiration. The overall effect of seasonality (i.e., "Season") presented a low ranking, as assessed through hypothesis testing. This finding justifies single tree use to classify predictors for PM samples from both the dry and the wet seasons.

Three main sources have influenced PM concentration at AF. These sources are represented through nodes 1, 2 and 4. Node 1 yielded to terminal node 7 – mean coarse particle mass (CPM) = $22 \mu g m^{-3}$, which is fully associated with dry season samples. The high BC content assigned to this terminal node reinforces the idea that biomass burning is a key factor to negatively modify air quality in AF.

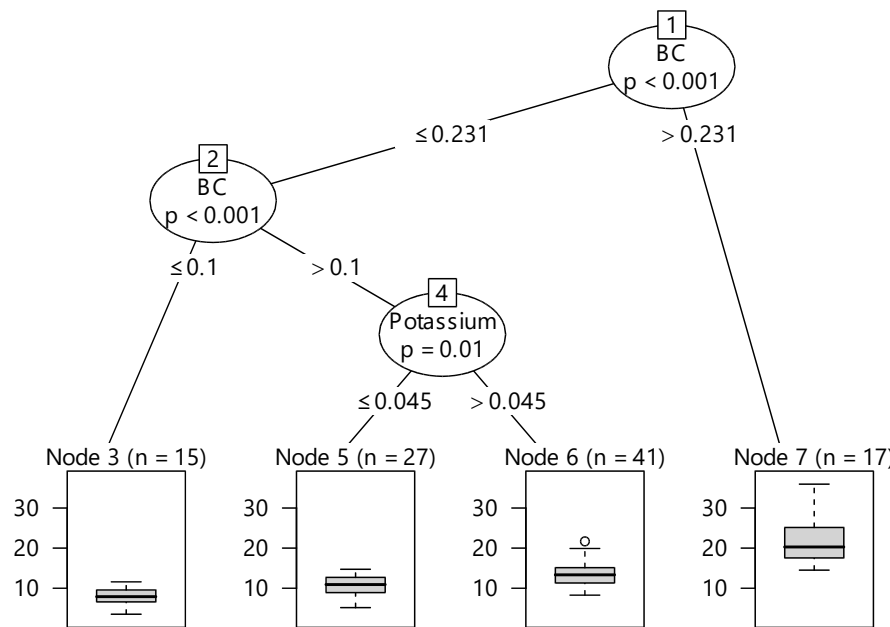


Figure 2. Conditional inference trees (CIT) for coarse mode aerosol data at Alta Floresta. In the CIT, n is the number of samples classified in a given node, and the coarse mode aerosol concentration is shown in the unit of $\mu g m^{-3}$.

Furthermore, the investigation of substructures in terminal node 7 points towards some degree of BC/ K⁺ correlation (Figure S4).

Node 4 yielded to terminal nodes 5 ($CPM_{[mean]} = 10.7 \mu\text{g m}^{-3}$) and 6 ($CPM_{[mean]} = 13.5 \mu\text{g m}^{-3}$). These two nodes share PO_4^{3-} related sources as a common feature. part in the coarse mode is often attributed to primary biological aerosol (PBA) in the Amazon Basin. Phosphorous has a good association with coarse mode, which was supported through different statistical analyses (Mahowald et al. 2005). We herein found a close association between PO_4^{3-} and K in terminal node 6 (Figure S5). There was little indicative of seasonality in PBA emissions if one considers the ratio of dry:wet season samples. However, PO_4^{3-} -related sources indicated by terminal node 5 presented higher dry season ratio samples than the wet season (Figure S6). Although reports on phosphorous losses during biomass burning are scarce, studies carried out *in situ* suggested approximately 60% loss (Mahowald et al. 2005).

Node 2 yielded to terminal node 3 ($CPM_{[mean]} = 7.9 \mu\text{g m}^{-3}$). Although this node presented the

lowest CPM, high sample rates were associated with the dry season. According to the HCA approach (Figure S6), there is statistical support for an association between PO_4^{3-} and coarse mode K⁺, as well as for formate and NH_4^+ . The association between PO_4^{3-} and coarse mode K⁺ can be ascribed to PBA, whereas organic ions balance ammonium in the fine and coarse fractions. It is typically more than enough in both the wet and the dry seasons, in the Amazon Basin (Martin et al. 2010).

Coarse Mode: Tangará da Serra

CIT consisted of 9 nodes, including 5 terminal nodes (Figure 3). BC concentration was the most important splitting variable for the root node, as observed at AF. Ranked below the BC, variables Ca^{2+} , formate and NO_3^- were also highly important. Variable "Season" was used as proxy indicator of low seasonality effect, based on the analysis of samples from dry and wet season in the same CIT. Therefore, there were three main sources influencing PM concentration at TS. These sources can be understood as the nodes

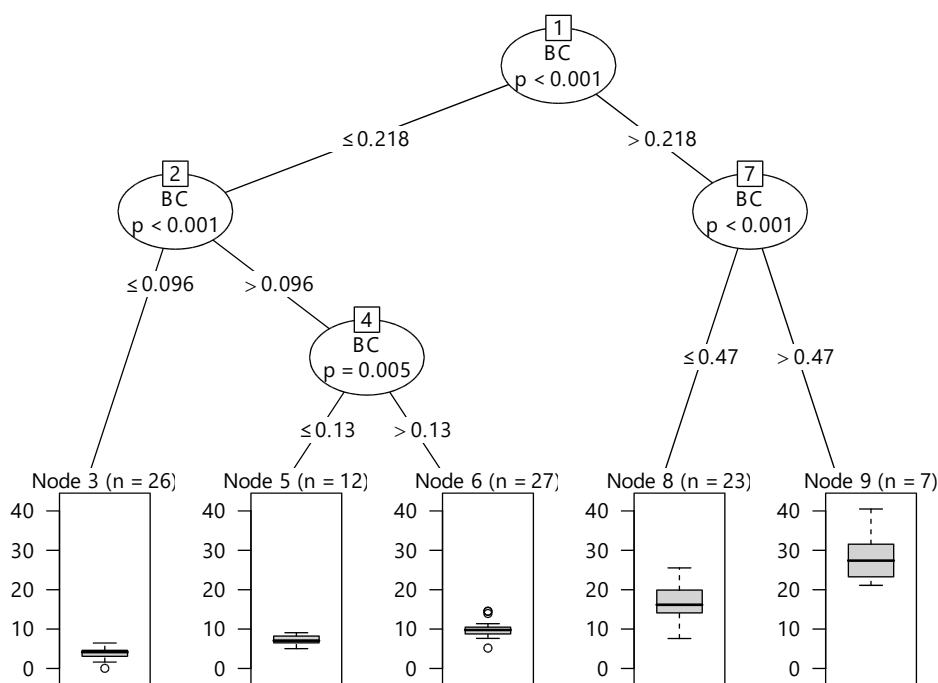


Figure 3. Conditional inference trees (CIT) for coarse mode aerosol data at Tangará da Serra. In the CIT, *n* is the number of samples classified in a given node, and the coarse mode aerosol concentration is shown in the unit of $\mu\text{g m}^{-3}$.

2, 4 and 7. Node 7 yielded to terminal nodes 9 ($CPM_{[mean]} = 28.4 \mu\text{g m}^{-3}$) and 8 ($CPM_{[mean]} = 16.9 \mu\text{g m}^{-3}$), which were associated with dry-season samples, alone. These two nodes were the ones associated with the highest BC content among TS samples. High BC can be linked to biomass burning. However, it is noteworthy that they present different chemical signatures (Figures S8 and S9).

Node 4 yielded to terminal nodes 6 ($CPM_{[mean]} = 9.9 \mu\text{g m}^{-3}$) and 5 ($CPM_{[mean]} = 7.3 \mu\text{g m}^{-3}$). These two nodes shared a close association between Mg^{2+} and Ca^{2+} (Figures S9 and S10). Dry and wet season sample ratios (# of dry season samples: # of wet season samples) recorded for terminal nodes 6 and 5 were 25:2 and 6:6, respectively. Furthermore, Mg^{2+} and Ca^{2+} in terminal node 6 was also associated (AU = 80) with BC (Figure S10), whereas the Mg^{2+} and Ca^{2+} in terminal node 5 was associated with variables resulting from PBA, such as PO_4^{3-} (Figure S11).

Node 2 yielded to terminal node 3 ($CPM_{[mean]} = 3.9 \mu\text{g m}^{-3}$). This terminal node presented equal dry and wet season sample ratios; it was also the one presenting the clearest days when it comes to mean coarse particle concentrations at TS.

However, there is a close association between coarse particle mass concentration and BC (Figure S13).

Coarse Mode: Manaus

CIT consisted of 7 nodes, including 4 terminal nodes (Figure 4). The two most important variables for coarse mode concentration prediction were Mg^{2+} and NO_3^- . As observed in AF and TS, the “Season” variable had little influence on coarse particle mass prediction. BC omission results from the technical difficulty to measure it. Three sources contributed to CPM; they were represented by nodes 1, 2 and 3. Node 1 yielded to terminal node 3 ($CPM_{[mean]} = 0.89 \mu\text{g m}^{-3}$), whose dry and wet season sample groups recorded the highest CPM values. Node 6 yielded to terminal node 6 ($CPM_{[mean]} = 0.34 \mu\text{g m}^{-3}$), which mostly held wet season sample groups. Based on HCA, associations between two sub-groups (including acetate and formate) were the most important patterns in this terminal node (Figure S14). Node 3 yielded to terminal nodes 5 ($CPM_{[mean]} = 0.17 \mu\text{g m}^{-3}$) and 4 ($CPM_{[mean]} = 0.10 \mu\text{g m}^{-3}$). Terminal node 5 was mainly represented by wet season samples and its chemical signature

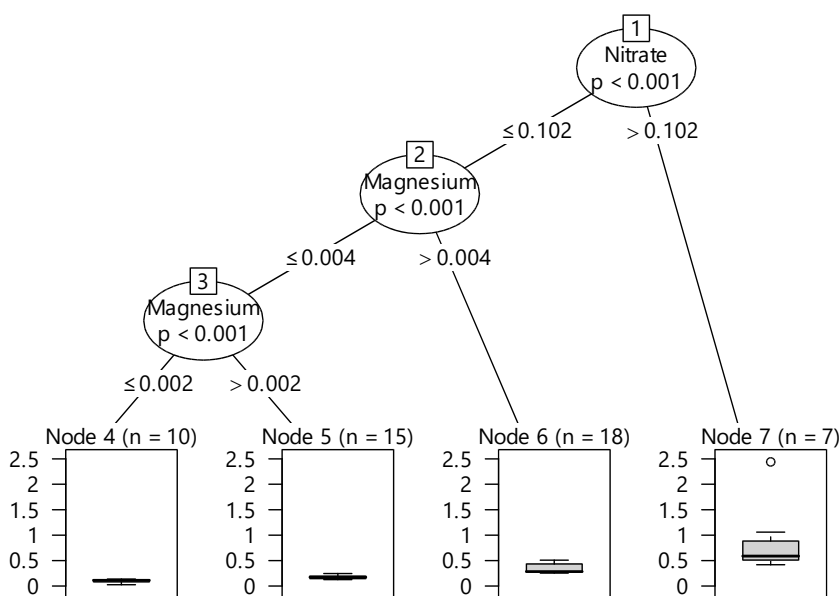


Figure 4. Conditional inference trees (CIT) for coarse mode aerosol data at Manaus. In the CIT, n is the number of samples classified in a given node, and the coarse mode aerosol concentration is shown in the unit of $\mu\text{g m}^{-3}$.

can be mostly related to PBA, due to the close association between $CPM - Ca^{2+}$ and $PO_4^{3-} - K^+$ (Figure S15). Terminal node 4, which was the one accounting for the lowest $CPM_{[mean]}$, presented a similar number of dry and wet season samples.

Fine Mode: Alta Floresta

CIT consisted of 11 nodes, including 6 terminal node (Figure 5). As observed for coarse mode samples, BC concentration was the most important splitting variable for the root node. The four most important variables to predict fine particle mass (FPM) were $BC > K^+ > Formate > NH_4^+$. The overall effect of seasonality (i.e., "Season") was low; only one CIT was applied to analyze all fine mode samples. Four main sources influenced fine mode PM concentration and they were represented by nodes 9, 2, 5 and 3. Nodes 9 and 2 mostly grouped dry season samples, whereas nodes 5 and 3 mostly grouped wet season samples. Node 9 yielded to terminal nodes 11 ($FPM_{[mean]} = 30.4 \mu g m^{-3}$) and 10 ($FPM_{[mean]} = 21.0 \mu g m^{-3}$). The first terminal node only grouped dry season samples, whereas the last node grouped 26 samples out of a total of 27. Although these two terminal nodes mostly grouped dry

season samples, rather than just $FPM_{[mean]}$, the chemical signature can be taken into account to assess the influence of biomass-burning sources (Figures S18 and S19). Surprisingly, HCA recorded for terminal node 11 indicated a sub-group with high AU; at first, it was composed by variables associated with the coarse mode (Figure S18). HCA recorded for terminal node 10 seemed equally complex with the association between K^+ and NH_4^+ was the most significant highlight (Figure S19). Node 2 yielded to terminal node 8 ($FPM_{[mean]} = 12.8 \mu g m^{-3}$). Samples grouped in this terminal node mostly regarded the dry season (14 out of 18). Although the overall importance of Ca^{2+} was not high in the fine fraction, there was clear evidence of Ca^{2+} , K^+ and NH_4^+ association (Figure S20). Such a finding can be associated with biomass burning.

Terminal nodes 7, 6 and 4 showed a similar characteristic, that is, the higher the number of wet season samples reflected in lower the $FPM_{[mean]}$. Node 5 yielded to terminal nodes 7 ($FPM_{[mean]} = 8.9 \mu g m^{-3}$) and 6 ($FPM_{[mean]} = 6.5 \mu g m^{-3}$). Terminal node 7 showed strong evidence of $NH_4^+ - SO_4^{2-} - K^+$, and $NO_3^- - Mg^{2+}$ associations (Fig. S21). This node may represent either a mix

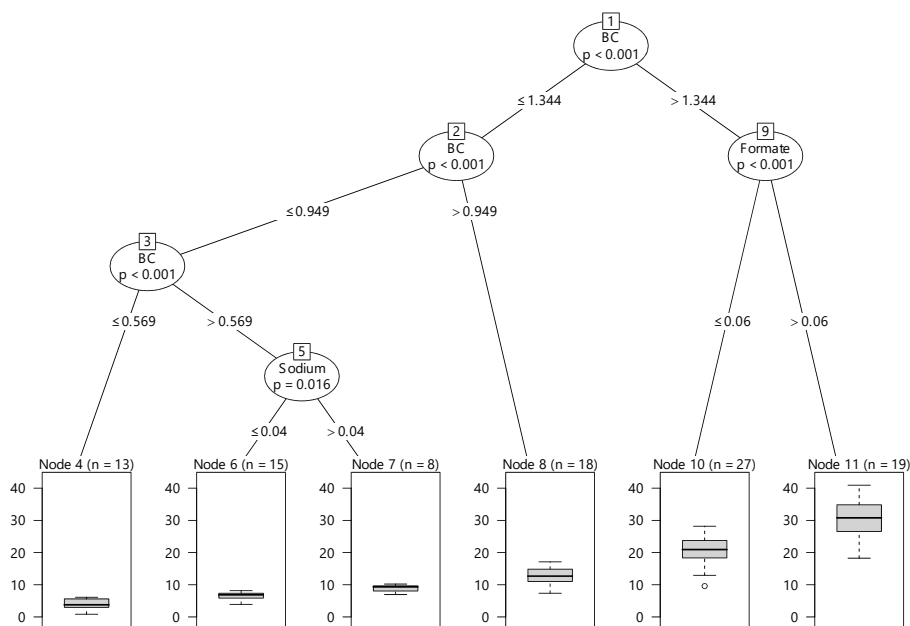


Figure 5. Conditional inference trees (CIT) for fine mode aerosol data at Alta Floresta. In the CIT, n is the number of samples classified in a given node, and the coarse mode aerosol concentration is shown in the unit of $\mu g m^{-3}$.

of sources or a transition between seasons since there was a slight difference between the number of wet and dry season samples. Node 3 yielded to terminal node 4 ($FPM_{[mean]} = 4.2 \mu\text{g m}^{-3}$), which presented the lowest BC concentration ($< 0.57 \mu\text{g m}^{-3}$) among all terminal nodes. This node grouped 11 wet season samples (out of 13), and such finding can be related to Amazon Basin background concentrations. According to the HCA analysis, the $\text{SO}_4^{2-} - \text{Ca}^{2+} - \text{FPM} - \text{K}^+ - \text{NH}_4^+$ association was strongly supported by the data collected herein.

Fine Mode: Tangará da Serra

CIT consisted of 11 nodes, including 6 terminal nodes (Figure 6). BC concentration was the most important splitting variable for the root node followed by formate, K^+ and NH_4^+ . BC and formate were key variables for both the coarse and fine modes. The overall importance of "Season" was, once again, very low. FPM concentration can be attributed to three main sources represented by nodes 9, 6 and 3. Node 9 yielded terminal nodes 11 ($FPM_{[mean]} = 35.0 \mu\text{g m}^{-3}$) and 10 ($FPM_{[mean]} = 23.0 \mu\text{g m}^{-3}$), which were associated with dry season

samples. Although terminal node 11 presented the highest $FPM_{[mean]}$, AU p-values recorded for terminal node 10 were more significant (Figures S24 and S25). Apart from differences between the two terminal nodes, both presented FPM – Formate, $\text{Mg}^{2+} - \text{Ca}^{2+}$ and $\text{NH}_4^+ - \text{SO}_4^{2-}$ associations. Therefore, terminal nodes 11 and 10 can be associated to biomass burning.

Node 6 yielded terminal nodes 8 ($FPM_{[mean]} = 15.0 \mu\text{g m}^{-3}$) and 7 ($FPM_{[mean]} = 10.4 \mu\text{g m}^{-3}$), which presented 10 and 25 dry season samples, respectively. Although terminal node 8 presented a lower number of dry season samples, it presented the highest BC content. With regard to chemical signatures, the two nodes were very similar (Figures S26 and S27).

Node 3 yielded terminal nodes 5 ($FPM_{[mean]} = 8.0 \mu\text{g m}^{-3}$) and 4 ($FPM_{[mean]} = 4.7 \mu\text{g m}^{-3}$), which presented 2 and 7 dry season samples, respectively. Terminal node 4 presented close FPM – BC association, as well as the lowest $FPM_{[mean]}$. This finding may suggest that either the biogenic aerosol-related samples (wet season) have light-absorbing features or the existence of small biomass burning.

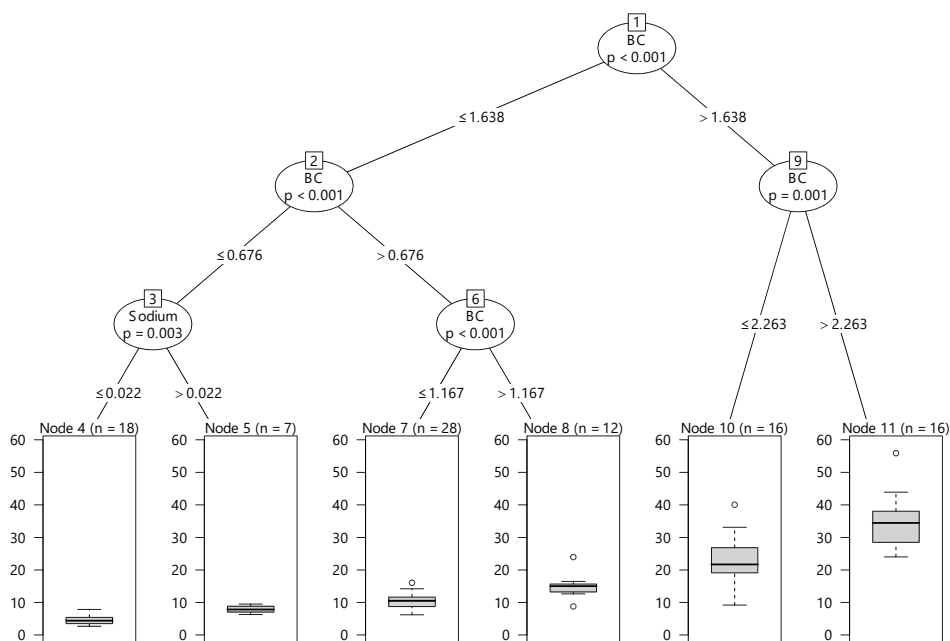


Figure 6. Conditional inference trees (CIT) for fine mode aerosol data at Tangará da Serra. In the CIT, n is the number of samples classified in a given node, and the coarse mode aerosol concentration is shown in the unit of $\mu\text{g m}^{-3}$.

Fine Mode: Manaus

CIT consisted of 5 nodes, including 3 terminal nodes (Figure 7). K^+ and SO_4^{2-} were the two most important variables for fine mode aerosol concentration prediction, followed by Mg^{2+} . Seasonality relevance as an FPM predictor in Manaus is a surprising finding taking into account the results obtained from AF and TS. Despite the technical difficulty to measure BC in Manaus, this observation may indicate environmental conservation at the site, since all CITs related to fine aerosol were more complex than the ones related to coarse aerosol, except for Manaus.

Two sources, represented by nodes 1 and 2, have contributed to FPM in Manaus. Node 1 yielded to terminal node 5 ($FPM_{[mean]} = 2.98 \mu g m^{-3}$), which mostly grouped dry season samples (7 out of 9). At least two distinct groups were presented in HCA in this terminal node, namely: one group more related to biogenic emissions and one group that seemed associated with biomass burning due to close $FPM - K^+$ association (Figure S30). Node 2 yielded to terminal nodes 4 ($FPM_{[mean]} = 1.42 \mu g m^{-3}$) and 3 ($FPM_{[mean]} = 0.63 \mu g m^{-3}$). The first one was mostly related to wet

season samples (21 out of 25) and the last one was closely related to the wet season. According to BP value, $Cl^- - NO_3^-$ and Acetate - Formate are the most important associations in terminal node 4 (Figure S31). The $Cl^- - NO_3^-$ association can represent important processes to turn HNO_3 into nitrate salts, such as reactions with ammonia, dust, and sea salt (Figure S32). On the other hand, the Acetate - Formate association may be related to the importance of biogenic volatile organic compounds (BVOCs) in the wet season. Terminal node 3 highlighted the importance of BVOCs in the wet season, as well as Acetate - Formate association, other biomass-burning tracers, and $SO_4^{2-} - NH_4^+ - FPM - K^+$ association (Figure S33). Basin wildfire events and Atlantic-transported pollution plumes are reasonable sources of particles in the wet season (Martin et al. 2010).

DISCUSSION

Regions where biomass burning is a constant activity are featured by high fine particle concentrations in comparison to the coarse ones, as observed in some Amazonian sites (Freitas et

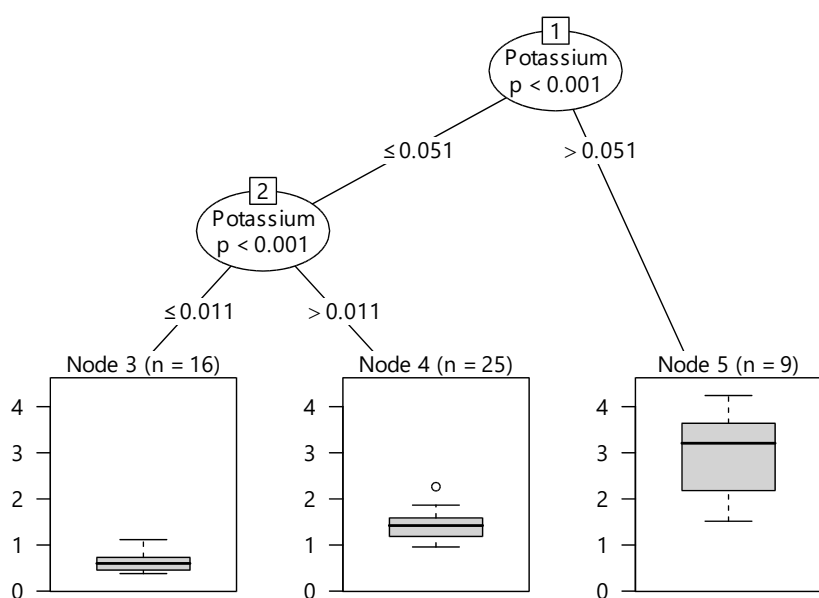


Figure 7. Conditional inference trees (CIT) for fine mode aerosol data at Manaus. In the CIT, n is the number of samples classified in a given node, and the coarse mode aerosol concentration is shown in the unit of $\mu g m^{-3}$.

al. 2005, Echalar et al. 1998). According to other PM studies carried out in the Amazon, there is compatibility of mean values recorded for concentrations of both fine and coarse particles if one considers that inorganic components corresponded to 10%-20% of the fine fraction, and the lower fraction thick rates (Martin et al. 2010).

The driest months, in their turn, are marked by higher PM concentrations, since biomass burning is more intense in all regions, including regions that are indirectly influenced by this practice happening elsewhere (e.g., Manaus). In addition, gold production accounts for particles' generation - it mostly happened in the 1980s and 1990s, in the AF region. However, over the last few decades, it was possible to observe these activities' depletion. This new scenario had a positive response on PM concentrations, mainly in the dry season since heavy rains make it difficult to work along the rivers. Manaus region showed the highest coarse particle concentrations in the rainy season, in comparison to the dry season, due to larger biogenic aerosols production. Thus, the presence of high coarse particle concentrations was associated with soil affected by fire events, mostly by fire outbreaks, whereas fine particles were linked to biomass burning.

Low BC concentrations was primarily found in Manaus region due to its environmental characteristics. Furthermore, the close correlation between BC and $PM_{2.0}$ confirmed the overall biomass origin of both pollutants. PM emitted during biomass burning is active cloud condensation nuclei (CCN), and it directly affects climate and precipitation patterns. The strong radioactive absorption properties of BC particles also drive climate change. It was confirmed through BC: $PM_{2.0}$ ratios in all assessed regions, that the amount of light absorbing material in

the atmosphere was statistically similar during the sampling period.

Potassium is a well-established biomass burning chemical marker (Galvão et al. 2019), given its volatility in the combustion process. Thus, K^+ concentration ratio between fine and coarse fractions is a proxy for fire events, so its enrichment in the fine fraction suggests the direct influence of biomass burning (Ryu et al. 2007). Correlations and mean ratios between BC and K^+ in the dry and rainy seasons confirmed biomass burning influence on PM chemical composition. However, high K^+ concentrations in coarse particles associated with the rainy season at both AF and TS indicate the contribution of biogenic aerosol emissions by plants, as observed in Manaus.

Low NO_3^- concentration and unfavorable conditions for NH_4NO_3 formation, such as high temperatures, justified the concentration values recorded for other substances accountable for making up the particles found in the Amazon.

SIA was associated with direct and indirect effects on climate change, such as the dispersion of yield solar radiation and acting as a CCN, respectively (IPCC, 2013). While SIA is a light-scattering species, BC is light-absorbing species, and it justifies the BC:SIA concentration ratio to better understand climate effects. The AF and TS regions showed the prevalence of light absorbing species (BC) over the light scattering ones (SIA) recorded for $PM_{2.0}$. The opposite was observed for $PM_{10-2.0}$. The comparison between effects from BC and SIA provided evidence of the most pronounced impacts of BC compared to SIA. It is so, because BC is an important fine aerosol fraction component, in addition to the fact that fine aerosol concentrations are higher than the coarser ones. Factors such as the long-term residence of fine aerosols in the atmosphere, likewise, their likelihood of

traveling long distances must also be taken into consideration in future analysis.

Regarding neutralization ratios, neither the sulfate nor the nitrate found in fine and coarse particles was neutralized by ammonium. Thus, the acidic properties presented by particles could increase their hygroscopicity, i.e., their ability to act as CCN, as well as the formation of secondary organic aerosols (Pathak et al. 2004, Zhang et al. 2007).

Furthermore, the low $\text{NO}_3^-:\text{SO}_4^{2-}$ ratio found in $\text{PM}_{2.0}$ in the dry season was associated with the fact that vehicle emissions were less important than other sources, such as biomass burning. However, the opposite result was recorded for $\text{PM}_{10-2.0}$.

The vegetation type observed in each of the assessed regions contributed to the differences found in particle concentrations. While tropical forest prevails in AF, TS showed Cerrado (Brazilian savannah) prevalence. Thus, $\text{PM}_{2.0}$ and BC concentrations were consistent with the determined emission factors, so much that higher BC emissions and fine particles could be observed in AF in biomass burning season in comparison to TS. However, other possible local sources may also have influenced PM chemical composition. Biogenic emissions, for example, contributed to Cl^- in both AF and TS. Oceanic air masses raised mean ion concentrations.

A balance between organic ions and ammonium, commonly observed in Amazon Basin's Atmospheric Chemistry explained the close formate and NH_4^+ association (Martin et al. 2010). The influence of biomass burning sources can be explained by the presence of K^+ and SO_4^{2-} , although low BC content, high ratio of rainy season samples and Ca^{2+} presence were mainly associated with biogenic emissions (Echalar et al. 1998, Santanna et al. 2016). There was a close association between chemical species, mainly in TS, due to processes of converting HNO_3 into

nitrate salts, the presence of biogenic volatile organic compounds and to biomass burning markers. Fires in the region and air masses from the Atlantic contributed to the composition of these particles.

Overall findings provided by CIT and Random Forests complied with other simpler techniques applied in the current study. However, we provided more robust solutions based on the interpretation of the last two algorithms, according to, at least, three groups: 1) dry season-associated samples, 2) wet season-associated samples; 3) groups that have provided the combination of both the dry and the wet seasons. Based on the HCA recorded for each node, in separate, further exploration revealed associations among variables, which were compared to previous studies carried out in the Amazon Basin.

CONCLUSIONS

PM, BC and WSI concentrations in fine and coarse fractions measured at AF and TS changed between seasons. The measured PM concentrations of the present study were lower than those measured in previous studies (from the 1990s and early 2000s). The lowest concentrations measured in 2008 derived from the smaller number of wildfire events detected at both sites. It has been observed noticeable biomass burning reduction since 2004, in AF. However, no reduction was observed in TS, since sugarcane production has been increasing in the last few decades.

Overall, PM, BC, and ion concentrations recorded the same order of magnitude in both AF and TS sites. Notably, there were significant differences amongst their characteristics, which suggest that the type of burned vegetation along with other sources may have influenced PM chemical composition. In our analysis,

SO₄²⁻ and BC have affected climate, with the latter suggesting more prominent effects. PM presented acidic features: SO₄²⁻ had more influence than NO₃⁻ or organic acids.

PM concentrations and most water-soluble inorganic ion species recorded higher concentrations in the dry season than in the wet season, in both size fractions (concentrations were approximately two to three times higher). K⁺, SO₄²⁻, SIA and BC were the most prominent components in the fine fraction, they presented close correlation amongst them, and such finding indicates biomass burning as the main associated source.

CIT, Random Forests and HCA based on multistep – multiscale bootstrap resampling – addressed an important part of intrinsic challenges faced by source apportionment in the Amazon Basin. The specific use and combination of these algorithms allowed us to study in more detail the relevance and relationship between the different variables that compose or may contribute to particles' mass and its further association with biomass burning seasons in these key sites.

Acknowledgments

This study was financed in part by the Coordenação de Aperfeiçoamento de Pessoal de Nível Superior – Brasil (CAPES) – Finance Code 001. The authors thank to Fundação de Amparo à Pesquisa do Estado do Rio de Janeiro (FAPERJ) and Conselho Nacional de Desenvolvimento Científico e Tecnológico (CNPq) for financial support. This paper is part of the INCT/CNPq project (Protocol No. 573797/2008-0), and of the Sub Climate-/FIOCRUZ network “Assessment of the Effects of Burning on Human Health in the Brazilian Amazon.” A. Gioda thanks FAPERJ for the Auxílio Cientista do Nosso Estado and CNPq for the Bolsa de Produtividade.

REFERENCES

ALBRECHT BA. 1989. Aerosols, Cloud Microphysics and Fractional Cloudiness. *Sci* 245: 1227-1230.

ANDREAE MO, ANDREAE TW, FERREK RJ & RAEMDONCK H. 1984. Long-range transport of soot carbon in the marine atmosphere. *Sci Total Environ* 36: 73-80.

ARANA A & ARTAXO P. 2014. Elemental composition of the atmospheric aerosol in the central Amazon basin. *Quím Nova* 37: 268-276.

ARIMOTO R, DUCE RA, SAVOIE DL, PROSPERO JM, TALBOT R, CULLEN JD, TOMZA U, LEWIS NF & JAY BJ. 1996. Relationships among aerosol constituents from Asia and the North Pacific during PEM-West A. *J Geophys Res Atmos* 101: 2011-2023.

ARTAXO P, BRUYNSEELS F, GRIEKEN RV & MAENHAUT W. 1988. Composition and sources of aerosol in the Amazon Basin. *J Geophys Res* 93: 1605-1615.

ARTAXO P, GERAB F, YAMASOE MA & MARTINS JV. 1994. Fine mode aerosol composition at three long-term atmospheric monitoring sites in the Amazon Basin. *J Geophys Res* 99: 22,857-22,868.

BOWEN HJM. 1979. *Environmental Chemistry of the Elements*. British Library. London: Academic Press, 362 p.

BREIMAN L. 2001. Random forests. *Mach Learn* 45: 5-32.

BULLOCK EL, WOODCOCK CE, SOUZA JUNIOR C & OLOFSSON P. 2020. Satellite-based estimates reveal widespread forest degradation in the Amazon. *Glob Chang Biol* 26: 2956-2969.

BUTT EW, CONIBEAR L, REDDINGTON CL, DARBYSHIRE E, MORGAN WT, COE H, ARTAXO P, BRITO J, KNOTE C & SPRACKLEN DV. 2020. Large air quality and human health impacts due to Amazon forest and vegetation fires. *Environ Res Commun* 2.

CAMMELLI F, GARRET RD, BARLOW J & PARRY L. 2020. Fire risk perpetuates poverty and fire use among Amazonian smallholders. *Glob Environ Chang* 63.

CARMO CN, HACON SS, LONGO KM, FREITAS S, IGNOTTI E, PONCE DE LEON A & ARTAXO P. 2010. Association between particulate matter from biomass burning and respiratory diseases in the southern region of the Brazilian Amazon. *Rev Panam Salud Publica* 27: 10-16.

COSTA MAM, AMARAL SS, NETO TGS, CARDOSO AA, SANTOS JC, SOUZA ML & JUNIOR CARVALHO JA. 2022. Forest Fires in the Brazilian Amazon and their Effects on Particulate Matter Concentration, Size Distribution, and Chemical Composition. *Combust Sci Technol* 194.

COVEY K ET AL. 2021. Carbon and Beyond: The Biogeochemistry of Climate in a Rapidly Changing Amazon. *Front For Glob Change* 4.

- DE OLIVEIRA H ET AL. 2022. Dynamics of Fire Foci in the Amazon Rainforest and Their Consequences on Environmental Degradation. *Sustainability* 14.
- ECHALAR F, ARTAXO P, MARTINS JV, YAMASOE M, GERAB F, MAENHAUT W & HOLBEN B. 1998. Long-term monitoring of atmospheric aerosols in the Amazon Basin' Source identification and apportionment. *J Geophys Res* 103: 849-864.
- FREITAS SR, LONGO KM, DIAS MAFS, DIAS PLS, CHATFIELD R, PRINS ED, ARTAXO P, GRELL GA & RECUERO FS. 2005. Monitoring the transport of biomass burning emissions in South America. *Environ Fluid Mech* 5: 135-167.
- GALVÃO ES, REIS NC, LIMA AT, STUETZ RM, ORLANDO MTD & SANTOS JM. 2019. Use of inorganic and organic markers associated with their directionality for the apportionment of highly correlated sources of particulate matter. *Sci Total Environ* 651: 1332-1343.
- HACON S, YOKOO E, VALENTE J, CAMPOS RC, SILVA VA, MENEZES ACC, MORAES LP & IGNOTTI E. 2000. Exposure to Mercury in Pregnant Women from Alta Floresta – Amazon Basin, Brazil. *Environ Res* 84: 204-210.
- HACON SS, ARTAXO P, GERAB F, YAMASOE MA, CAMPOS RC, CONTI LF & DE LACERDA LD. 1995. Atmospheric mercury and trace elements in the region of Alta Floresta in the Amazon basin. *Water Air Soil Pollut* 80: 273-283.
- HOTHORN T, BUHLMANN P, DUDOIT S, MOLINARO A & LAAN MJ. 2005. Survival ensembles. *Biostat* 7: 355-373.
- HOTHORN T, HORNIK K & ZEILEIS A. 2006. Unbiased recursive partitioning: a conditional inference framework. *J Comput Graph Statistics* 15: 651-674.
- IGNOTTI E, HACON SS, JUNGER WL, MOURAO D, LONGO KM, FREITAS S, ARTAXO P & PONCE DE LEON AC. 2010. Air pollution and hospital admissions for respiratory diseases in the subequatorial Amazon: a time series approach. *Cad Saude Publica* 26: 747-761.
- IPCC - INTERGOVERNMENTAL PANEL ON CLIMATE CHANGE. 2013. *Climate Change In: Houghton JT, Meira Filho LG, Gallander BA, Harris N, Kattenberg A & Maskell K (Eds), Cambridge University Press, Cambridge.*
- LACERDA LD, SOUZA M & RIBEIRO MG. 2004. The effects of land use change on mercury distribution in soils of Alta Floresta, Southern Amazon. *Environ Pollut* 129: 247-255.
- LIU Y & DAUM PH. 2002. Indirect warming effect from dispersion forcing. *Nature* 419: 580-581.
- MAENHAUT W, CAFMEYER J, RAJTA I, KUBAHTOVAH A & CLAEYS M. 1998. Aerosol chemistry at Balbina, Brazil, during LBA-CLAIRE-98. *EOS Transactions of the American Geophysical Union* 79(Suppl.): F155-F156.
- MAENHAUT W, FERNANDEZ-JIMENEZ MT, RAJTA I & ARTAXO P. 2002. Two-year study of atmospheric aerosols in Alta Floresta, Brazil: Multielemental composition and source apportionment. *Nucl Instrum Methods Phys Res Section B: Beam Interactions with Materials and Atoms* 189: 243-248.
- MAHOWALD NM, ARTAXO P, BAKER AR, JICKELLS TD, OKIN GS, RANDERSON JT & TOWNSEND AR. 2005. Impacts of biomass burning emissions and land use change on Amazonian atmospheric phosphorus cycling and deposition. *Glob Biogeochem Cycles* 19.
- MARTIN ST ET AL. 2010. Sources and properties of Amazonian aerosol particles. *Rev Geophys* 48.
- PALAREA-ALBALADEJO J & MARTIN-FERNANDEZ JA. 2015. zCompositions — R package for multivariate imputation of left-censored data under a compositional approach. *Chemom Intell Lab Syst* 143: 85-96.
- PATHAK RK, LOUIE PKK & CHAN CK. 2004. Characteristics of aerosol acidity in Hong kong. *Atmos Environ* 38: 2965-2974.
- R DEVELOPMENT CORE TEAM. 2013. R: a Language and Environment for Statistical Computing. R Foundation for Statistical Computing, Vienna, Austria. <<http://www.R-project.org/>>, <http://www.R-project.org>. (accessed October 2014).
- ROCHA R & SANT'ANNA AA. 2022. Winds of fire and smoke: Air pollution and health in the Brazilian Amazon. *World Dev* 151.
- RYU SY, KWON BG, KIM YJ, KIM HH & CHUN KJ. 2007. Characteristics of biomass burning aerosol and its impact on regional air quality in the summer of 2003 at Gwangju, Korea. *Atmos Res* 84: 362-373.
- SANTANNA FB, ALMEIDA FILHO EO, VOURLITIS GL, ARRUDA PHZ, PALACIOS RS & NOGUEIRA JS. 2016. Elemental composition of PM10 and PM2.5 for a savanna (cerrado) region of Southern Amazonia. *Quím Nova* 39: 1170-1176.
- SILVA RDO, BARIONI LG & MORAN D. 2021. Fire, deforestation and livestock: When the smoke clears. *Land Use Policy* 100.
- STROBL C, BOULESTEIX AL, KNEIB T, AUGUSTIN T & ZEILEIS A. 2008. Conditional Variable Importance for Random Forests. *BMC Bioinform* 9: 307.
- STROBL C, BOULESTEIX AL, ZEILEIS A & HOTHORN T. 2007. Bias in random forest variable importance measures:

Illustrations, sources and a solution. BMC Bioinform 8: 25.

SUZUKI R & SHIMODAIRA H. 2006. Pvcust: an R package for assessing the uncertainty in hierarchical clustering. Bioinform 22: 1540-1542.

TAKEISHI A, STORELMO T & FEROZ L. 2020. Disentangling the Microphysical Effects of Fire Particles on Convective Clouds Through A Case Study. J Geophys Res Atmos 125.

TWOMEY S. 1959. The nuclei of natural cloud formation part II: The supersaturation in natural clouds and the variation of cloud droplet concentration. Pure Appl Geophys 43: 243-249.

URRUTIA-PEREIRA M, RIZZO LV, CHONG-NETO HJ & SOLE D. 2021. Impact of exposure to smoke from biomass burning in the Amazon rain forest on human health. J Bras Pneumol 47.

ZHANG Q, JEMENEZ JL, WORSNOP DR & CANAGARATNA M. 2007. A case study of urban particle acidity and its influence on secondary organic aerosol. Environ Sci Technol 41: 3213-3219.

SUPPLEMENTARY MATERIAL

Figure S1-S32.

How to cite

GIODA A ET AL. 2023. Assessing over decadal biomass burning influence on particulate matter composition in subequatorial Amazon: literature review, remote sensing, chemical speciation and machine learning application. An Acad Bras Cienc 95: e20220932. DOI 10.1590/0001-3765202320220932.

*Manuscript received on October 21, 2022;
accepted for publication on April 5, 2023*

ADRIANA GIODA¹

<https://orcid.org/0000-0002-5315-5650>

VINICIUS L. MATEUS¹

<https://orcid.org/0000-0002-7732-6207>

SANDRA S. HACON²

<https://orcid.org/0000-0002-8222-0992>

ELIANE IGNOTTI³

<https://orcid.org/0000-0002-9743-1856>

RUAN G.S. GOMES¹

<https://orcid.org/0000-0002-1376-0995>

MARCOS FELIPE S. PEDREIRA¹

<https://orcid.org/0000-0002-5755-7438>

JOSÉ MARCUS GODOY¹

<https://orcid.org/0000-0001-6135-090X>

RIVANILDO DALLACORT⁴

<https://orcid.org/0000-0002-7634-8973>

ANA LÚCIA M. LOUREIRO⁵

<https://orcid.org/0009-0009-2773-1181>

FERNANDO MORAIS⁵

<https://orcid.org/0000-0002-7207-4450>

PAULO ARTAXO⁵

<https://orcid.org/0000-0001-7754-3036>

¹Pontifical Catholic University of Rio de Janeiro (PUC-Rio), Department of Chemistry, Rua Marques de São Vicente 225, Gávea, 22451-900 Rio de Janeiro, RJ, Brazil

²Oswaldo Cruz Foundation, National School of Public Health, Rua Leopoldo Bulhões, 1480, Manguinhos, 21041-210 Rio de Janeiro, RJ, Brazil

³State University of Mato Grosso, Avenida São João, 563, Bairro Cavalhada I, 78216-060 Cáceres, MT, Brazil

⁴State University of Mato Grosso, Avenida Inácio Bittencourt, 6967, Bairro Jardim Aeroporto, 78300-000 Tangará da Serra, MT, Brazil

⁵University of São Paulo, Institute of Physics, Rua do Matão 1371, Cidade Universitária, 05508-090 São Paulo, SP, Brazil

Correspondence to: **Adriana Gioda**

E-mail: agioda@puc-rio.br

Author contributions

Adriana Gioda - works on paper design, data interpretation, writing, and review. Vinicius Lionel Mateus - worked on data interpretation applying Machine Learning. Sandra de Souza Hacon - get funds for the project and reviewed the article. Eliane Ignotti - get funds for the project and reviewed the article. Ruan Gonçalves de Souza Gomes - worked on data interpretation and reviewed the article. Marcos Felipe de Souza Pedreira - article adjustments and review. José Marcus Godoy - chemical analysis. Rivanildo Dallacort - sample collection and article review. Fernando Moraes - sample collection and article review. Paulo Artaxo - get funds for the project and sample collection.

